
CHATCFD: AN END-TO-END CFD AGENT WITH DOMAIN-SPECIFIC STRUCTURED THINKING

E Fan², Weizong Wang^{1,3}, and Tianhan Zhang^{1,3,4,*}

¹School of Astronautics, Beihang University

²Department of Mechanics and Aerospace Engineering, Southern University of Science and Technology

³Key Laboratory of Spacecraft Design Optimization and Dynamic Simulation Technology, Ministry of Education

⁴Beijing Key Laboratory of High Efficiency Spacecraft Propulsion Technology

*Corresponding author, thzhang@buaa.edu.cn

ABSTRACT

Computational Fluid Dynamics (CFD) is critical for scientific and engineering advancements but is hindered by operational complexity and the need for extensive domain expertise. This paper presents ChatCFD, a large language model (LLM)-driven pipeline that automates computational fluid dynamics (CFD) workflows within the OpenFOAM framework, enabling users to configure and execute complex simulations from natural language prompts or published literature with minimal prior expertise. A key innovation is its ability to think structurally in database construction, configuration validation, and error reflection, which systematically integrates domain-specific CFD and OpenFOAM knowledge (e.g., solvers, turbulence models, file dependencies) with general LLMs, thereby enhancing accuracy and adaptability. More specifically, ChatCFD employs a four-stage workflow: (1) Knowledge Base Construction, creating a structured JSON database from OpenFOAM tutorials and manuals; (2) User Input Processing, guiding users via a multimodal interface (dialogue, documents, mesh files); (3) Case File Initialization, generating case files using a preprocessed knowledge base; and (4) Simulation Execution and Error Correction, running simulations and resolving errors with Retrieval-Augmented Generation (RAG). Powered by DeepSeek-R1 and DeepSeek-V3 models, a multi-agent architecture, and specialized OpenFOAM knowledge, ChatCFD features an interactive chat interface, hierarchical parameter extraction, and a robust error correction system addressing dimension mismatches, missing files, persistent errors, and general issues. Validation results demonstrate that ChatCFD autonomously reproduces published CFD literature results without human intervention, a challenging task involving complex, unseen configurations beyond basic CFD examples and general LLM capabilities. This achievement underscores the significant advancement enabled by its domain-specific structured thinking ability. In addition, validation experiments demonstrate error-free configurations in 30-40% of incompressible and compressible CFD cases and operational success in 60-80%, establishing a benchmark for automated CFD. By reducing expertise barriers, ChatCFD enhances CFD accessibility and provides methodological insights for AI-driven engineering simulations.

github: The code for ChatCFD is available at: <https://github.com/EarlFan/ChatCFD>.

Keywords large language model, multi-agent system, computational fluid dynamics, automated CFD

1 Introduction

Computational Fluid Dynamics (CFD) is a cornerstone technology in diverse scientific and engineering disciplines, including aerospace [28, 14, 12], energy systems [17, 2], urban environment [22, 19, 27], combustion [26, 10, 11], and biomedical applications [24, 9, 7]. It provides indispensable tools for simulating intricate fluid behaviors, thereby enabling design innovation and scientific discovery [3, 4]. However, the practical deployment of CFD faces significant challenges. Traditional CFD simulations require extensive domain-specific expertise [32] and frequently rely on costly commercial software packages. Even experienced engineers must invest considerable time in critical tasks, including

solver selection, model development, mesh generation, boundary condition specification, and post-processing[20]. These complexities, compounded by the substantial computational resources needed, restrict the broader adoption of CFD, particularly for smaller enterprises and research groups, thus creating high entry barriers and potentially stifling innovation [4]. Consequently, there is a critical need for automated, user-friendly, and cost-effective CFD tools. To address this, we introduce ChatCFD, an automated agent system that leverages advanced artificial intelligence to streamline the CFD workflow.

Recent advances in Artificial Intelligence (AI) have revolutionized the automation landscape of complex scientific workflows. At the forefront of this transformation are Large Language Models (LLMs)—including GPT [1], Gemini [30], and DeepSeek [13]—alongside advanced multi-agent frameworks such as MetaGPT [15], and AutoGen [34]. These LLMs exhibit remarkable proficiency in natural language understanding, code generation, and complex reasoning tasks through chain-of-thought processes [33], enabling the development of autonomous LLM-based agents that can effectively perceive, reason, and act within their operational environment. Furthermore, the integration of Retrieval-Augmented Generation (RAG) [21] significantly enhances these agents. RAG is a technique where, before generating a response or performing an action, the LLM retrieves relevant information from an external, often domain-specific, knowledge base. This retrieved context is then provided to the LLM to inform its output. This process strengthens agents by grounding their responses in factual data, reducing hallucinations, and enabling them to perform more effectively in specialized domains like CFD.

This technological convergence has catalyzed the development of powerful LLM-based agents capable of automating the CFD workflow spectrum, from interpreting natural language specifications to configuring and executing simulations. This advancement represents a significant step toward making complex CFD simulations more accessible and efficient. OpenFOAM [18], in particular, stands out as the most popular open-source and free CFD software package, whose extensive capabilities, flexible architecture, and vibrant community support have made it a preferred choice for academic research, industrial applications, and consequently, a common framework for developing novel CFD automation agents. This accessibility has fostered innovation, leading to several pioneering initiatives exploring the integration of LLMs within the CFD domain. For example, MetaOpenFOAM [5] was introduced as an LLM-based multi-agent framework utilizing the MetaGPT [15] paradigm and RAG to automate CFD simulation tasks from natural language inputs, primarily demonstrated with OpenFOAM tutorial cases. Concurrently, OpenFOAMGPT [25] explored RAG-augmented LLM agents for OpenFOAM-centric CFD simulations, assessing model proficiency in tasks like zero-shot case setup and boundary condition adjustments. Foam-Agent [23] further advanced this area by proposing a multi-agent system with innovations such as hierarchical multi-index retrieval and dependency-aware file generation. Other research avenues have concentrated on fine-tuning LLMs with domain-specific datasets, like NL2FOAM [8], to enhance direct translation from natural language to executable CFD configurations, potentially using techniques like LoRA [16]. Despite these significant strides in automating CFD pipeline components and reducing technical barriers, existing systems often struggle with the end-to-end management of complex simulations without human intervention.

Existing CFD automation agents are often limited by their focus on rudimentary tasks, typically restricted to OpenFOAM tutorial-level examples, raising concerns about their generalization to complex, unseen cases. Three critical challenges remain unaddressed. First, describing CFD cases using brief natural language is often inadequate, as practical simulations require precise specifications beyond simplified verbal descriptions. If not given a detailed and professional task description, effective agents must interactively clarify user intent to define simulation requirements accurately. Second, handling intricate geometries poses significant difficulties, as mesh generation for real-world scenarios exceeds the capabilities of basic OpenFOAM utilities like “bLockMesh” and demands specialized meshing tools. The inability to integrate user-defined or externally generated meshes limits these agents’ utility for diverse, practical CFD problems. Third, incorporating domain-specific knowledge into CFD agents remains challenging. Engineering-scale simulations require comprehensive initial and boundary condition specifications, necessitating domain-specific structural thinking and seamless integration of specialized domain expertise into the automation pipeline. These shortcomings highlight a critical gap in current CFD automation frameworks.

To address the limitations outlined above, this paper introduces ChatCFD, an automated agent system for configuring and executing CFD simulations within the OpenFOAM framework, as illustrated in Fig. 1. ChatCFD enables users to define cases interactively via a chat interface or by uploading detailed technical files, such as well-documented research papers. Leveraging large language models (e.g., DeepSeek-R1, DeepSeek-V3), a sophisticated multi-agent architecture, and specialized OpenFOAM knowledge, ChatCFD autonomously manages the entire simulation workflow. It adeptly handles complex CFD setups through iterative trial-and-error, supporting comprehensive initial and boundary conditions, intricate physical models, and user-defined or externally generated mesh files. This architecture enables ChatCFD to address diverse, unseen scenarios and adapt various physical models, marking a significant advancement over prior agents.

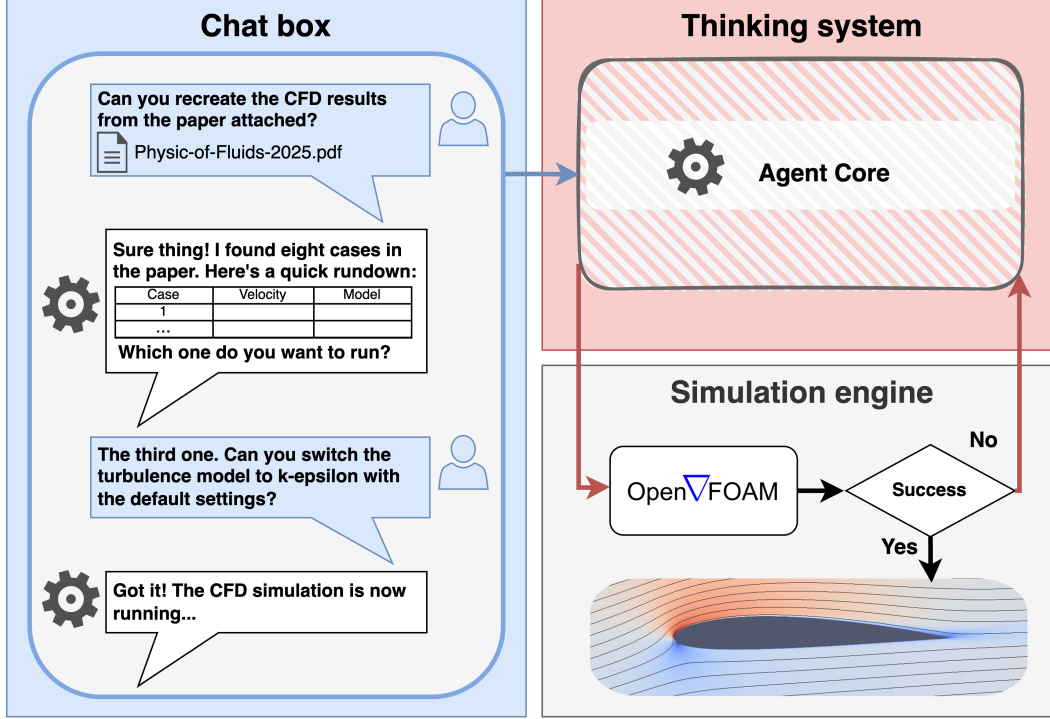


Figure 1: Overview of the ChatCFD automated agent system for streamlining CFD simulations within the OpenFOAM framework. ChatCFD enables researchers and engineers to configure and execute simulations with minimal CFD or OpenFOAM expertise. The system comprises three core components: (1) an interactive chat interface for users to input case descriptions or upload mesh files, (2) a thinking system, the core decision-making module (detailed in Figure 2), and (3) a simulation engine that executes cases, collects error logs, and delivers final results.

This paper presents the detailed architecture of the ChatCFD system and validates its modular effectiveness through experimental analysis. The paper is organized as follows: Section 2 details the system architecture, Section 3 provides experimental results demonstrating the effectiveness of its components, and Section 4 summarizes the key findings. An appendix includes illustrative examples and prompts to clarify ChatCFD’s operational functionality.

2 Method

ChatCFD is an automated CFD agent system that leverages the OpenFOAM framework to process multi-modal user inputs, including research articles and mesh files, to configure and execute CFD simulations based on user instructions. As illustrated in Fig. 2, the ChatCFD framework implements a comprehensive workflow to streamline simulation setup, execution, and analysis.

2.1 Stage 0: Knowledge Base Construction

The preprocessing aims to establish a foundational knowledge base for CFD tasks, performed in advance to optimize ChatCFD’s operations. Ideally, this knowledge base contains general CFD principles (e.g., numerical differentiation, discretization schemes), OpenFOAM-specific manuals, and a comprehensive example library. Fine-tuning large language models (LLMs) for general CFD knowledge is beyond the current scope; readers are referred to recent work by Dong et al. [8]. This study focuses on preprocessing OpenFOAM manuals and tutorials constructs a structured JSON database, cataloging essential parameters such as solver configurations, turbulence models, and file dependencies, providing a critical foundation for accurate case setup and error correction.

Initially, preprocessed manual and tutorial data define the file dependency relationship, accessed during the RAG process to enhance the agent’s error correction ability. To ensure robust operation, strategic case filtering is implemented, removing OpenFOAM-specific headers, excluding cases with external dependencies or auxiliary folders to maintain

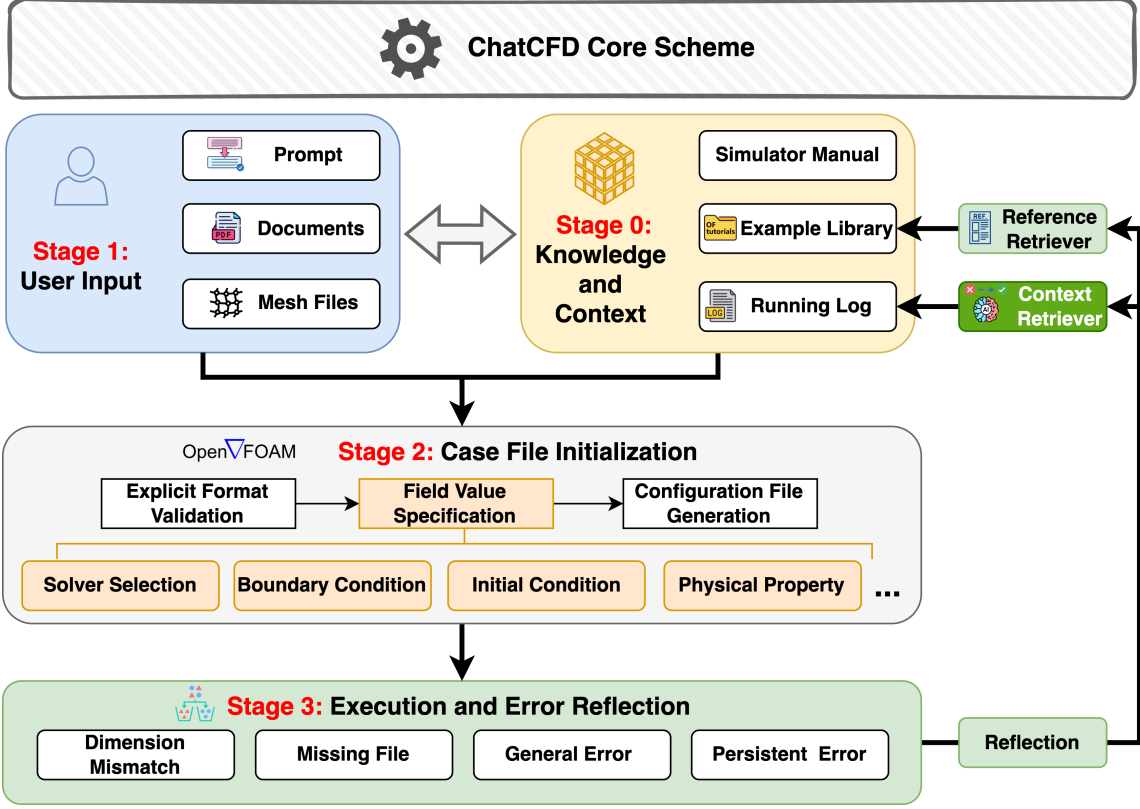


Figure 2: Architecture of the ChatCFD framework for automated CFD simulations, illustrating the four-stage workflow and agent structure. The stages are: (1) Knowledge Base Construction, creating a JSON database from OpenFOAM manuals and tutorials; (2) User Input Processing, enabling user interaction via natural language or document and mesh uploads; (3) Case File Initialization, running simulations, generating OpenFOAM case files using the knowledge base; and (4) Simulation Execution and Error Reflection, converting meshes with `fluentMeshToFoam`, and resolving errors (dimension mismatches, missing files, persistent errors, general issues) using RAG-based modules `ReferenceRetriever` and `ContextRetriever`. The agent structure integrates DeepSeek-R1 and DeepSeek-V3 for intelligent processing, with iterative error correction.

independence, and filtering out cases with extensive non-uniform field definitions that reduce LLM response quality without contributing to configuration. Filtering criteria and implementation details are provided in Appendix A.

Subsequently, the example library is preprocessed through systematic extraction and organization. All case configuration files are parsed and converted into a structured JSON format, tagged with metadata such as solver specifications, turbulence model types, and flow regime characteristics. Analysis of solver and turbulence model distributions determines specific file requirements for each configuration. For instance, the `simpleFoam` solver requires configuration files including `system/fvSolution`, `system/controlDict`, `system/fvSchemes`, `0/p`, `0/U`, `constant/transportProperties`, and `constant/turbulenceProperties`. Similarly, the `kOmegaSST` turbulence model requires `system/fvSolution`, `system/controlDict`, `system/fvSchemes`, `0/p`, `0/U`, `0/k`, `0/omega`, `0/nut`, `constant/turbulenceProperties`, and `constant/transportProperties`.

2.2 Stage 1: User Input Processing

The initial stage of ChatCFD features an interactive, multi-modal interface that enables users to define CFD simulations by either conversing with the DeepSeek-R1 model or uploading documents and mesh files, built using the Streamlit Python framework. This interface leverages the preprocessed knowledge base to facilitate accurate case specification with minimal CFD expertise. The knowledge base, comprising OpenFOAM manuals, tutorial cases, and a structured JSON database of solver configurations and turbulence models, informs the system’s natural language processing and case extraction, ensuring robust and context-aware interactions. The workflow comprises four key phases:

- **Input Submission:** Users can upload research articles or describe the case through dialogue to provide the basis for case analysis.
- **Case Extraction:** The system extracts and catalogs CFD cases from uploaded documents or conversation inputs, identifying solver configurations and physical models, and presents them in a structured format with unique identifiers (e.g., Case 1, Case 2).
- **Case Selection:** Through natural language interaction, the system guides users to select a target case, provides detailed specifications for verification, and confirms the selection.
- **Mesh Integration:** The system assists users in uploading mesh files, currently supporting Fluent-format .msh files.

Upon completing this workflow, ChatCFD aggregates three essential components for downstream processing, as shown in Fig. 2:

- **Case Documentation:** The system retains the full research article or conversation details, providing access to all technical specifications, including solvers, boundary conditions, and simulation parameters.
- **Case Specification:** The selected case is recorded with detailed metadata, including solver types, numerical schemes, physical models, and source references, ensuring precise setup.
- **Mesh Data:** Robust file transfer and path management ensure reliable delivery of mesh data to subsequent stages.

2.3 Stage 2: Case File Initialization

The CFD engineer layer, powered by the DeepSeek-R1 model, initializes OpenFOAM case files through a streamlined two-phase process, leveraging the preprocessed knowledge base.

In the first phase, the system generates a configuration list of required case files by analyzing the case description from Stage 1 to determine the appropriate solver and turbulence model. It queries the knowledge base’s OpenFOAM dataset to compile a tailored list of necessary files (e.g., `system/fvSolution`, `0/p`) for the solver-turbulence model pair, enhancing initialization accuracy and minimizing missing file errors. Such a procedure, based on an explicit manner, substantially enhances the quality of case file initialization and reduces the incidence of missing file errors.

The second phase extracts detailed case setups from three sources: the configuration list, user prompt, and example library. The configuration list ensures precise case identification, while the prompt is segmented by section and filtered using the `sentence-transformers/all-mpnet-base-v2` library with relevance thresholds. Hierarchical parameter extraction follows three steps:

- **Boundary Condition Validation:** The system identifies boundary types from the prompt, verifies compatibility with OpenFOAM v2406, and enforces strict naming conventions to avoid errors. For example, in the airfoil case shown in Fig. 3, while the LLM may default to using a generic “inlet” type for the Inlet boundary based on common practice, the system ensures it correctly implements the specified “freeStream” boundary condition type to maintain fidelity with the original case setup.
- **Field Value Specification:** Initial and boundary condition values are extracted for all field files (e.g., `0/p`, `0/nut`, `0/nutIlda`) listed in the configuration.
- **Configuration File Generation:** All required OpenFOAM files are generated, including field files (`0/`), physical properties (`constant/`, excluding `polyMesh/`), and control parameters (`system/`).

Step 3 leverages DeepSeek-R1’s reasoning capabilities to orchestrate the simultaneous generation of all required case configuration files while ensuring consistency across physical models and boundary conditions. For numerical configurations not explicitly specified in the research article, such as discretization schemes and solution algorithms defined in `system/fvSchemes` and `system/fvSolution` files, ChatCFD employs DeepSeek-R1’s advanced reasoning capabilities to construct appropriate configurations based on its understanding of CFD best practices and the physical requirements of the case. The agent maintains coherence between interdependent parameters while adapting numerical schemes to match the flow physics and solution requirements indicated by the article’s methodology.

2.4 Stage 3: Simulation Execution and Error Reflection

Stage 3 executes the CFD simulation and analyzes runtime logs for automated error correction through three sequential steps:

- **Case Deployment:** Case files from Stage 2 are deployed to the designated directory, and uploaded mesh files are converted to OpenFOAM format using `fluentMeshToFoam`, storing results in `constant/polyMesh`.

- **Temporal Configuration:** Temporal parameters in `system/controlDict` are set, running 10 iterations/time steps for steady-state or transient simulations, with outputs at steps 0, 5, and 10. Transient cases enforce a maximum CFL number of 0.6, with time steps of 1×10^{-5} s for incompressible flows and 1×10^{-8} s for compressible flows.
- **Simulation Execution:** The simulation runs using the specified OpenFOAM solver, with execution output logged to `case_run.log` for analysis.

ChatCFD automates error detection and correction in OpenFOAM case files by analyzing runtime logs using RAG and two retrieval modules:

The `ReferenceRetriever` module queries the preprocessed OpenFOAM knowledge database to select reference case files with matching or similar solvers and physical configurations. Typically, three reference files balance guidance and prompt complexity, ensuring contextually relevant corrections (e.g., distinguishing incompressible vs. compressible flows).

The `ContextRetriever` module compiles all current case configurations into a structured JSON format, providing the DeepSeek-V3 model with comprehensive context to address errors like missing files, especially in physically coupled problems (Section 3.3).

Upon detecting a runtime error, ChatCFD classifies it into four categories, detailed in Appendix B with examples:

- **Dimension Mismatches:** Inconsistent physical dimensions in field or configuration files are identified by DeepSeek-V3 through log pattern analysis. Corrections involve adjusting dimensions to match reference files from `ReferenceRetriever`, ensuring consistency.
- **Missing Files:** Missing case files, as reported in MetaOpenFOAM [5], are detected via log messages. DeepSeek-V3 identifies the missing file, `ReferenceRetriever` provides a template, and `ContextRetriever` supplies existing case details. DeepSeek-R1 generates the file, ensuring consistency in boundary patches, dimensions, and solver settings.
- **Persistent Errors:** Errors recurring across correction cycles are tracked by DeepSeek-R1. The problematic file is identified, and DeepSeek-V3 rewrites it using reference files from `ReferenceRetriever` and the original file content.
- **General Errors:** Errors like incorrect keywords or numerical schemes, comprising 50% of runtime issues, are addressed through a three-step process:
 - **Error Localization:** DeepSeek-R1 analyzes the log and case files (via `ContextRetriever`) to pinpoint the erroneous file, constraining the search to relevant files to reduce LLM errors.
 - **Correction Proposal:** DeepSeek-R1 generates step-by-step correction advice using the error log, erroneous file, and reference files from `ReferenceRetriever`, preserving initial and boundary conditions from Stage 1.
 - **Correction Application:** DeepSeek-V3 applies the correction, adhering to the advice and maintaining dimensional consistency.

2.5 LLM Configurations

ChatCFD employs a dual-model approach, integrating DeepSeek-R1 and DeepSeek-V3 to handle the initiation and correction of case files in the workflow. The application of these two LLMs follows distinct principles. DeepSeek-R1 takes the lead in Stage 2, where it extracts comprehensive case setups from textual descriptions and configures the initial case files. Its capacity for in-depth text comprehension and error correction is also crucial in Stage 3, where it analyzes and rectifies general errors and generates any missing files. DeepSeek-V3’s contributions are concentrated in Stage 3, focusing on the correction of case files. It excels at managing highly patterned tasks, such as identifying dimensional and file-missing errors. Furthermore, DeepSeek-V3 handles specific corrections, such as adjusting field file dimensions, rebuilding case files to correct persistent errors, and amending files according to precise step-by-step instructions.

This synergistic use of DeepSeek-R1 and DeepSeek-V3 significantly enhances ChatCFD’s overall performance, particularly in correcting case files. While DeepSeek-R1 excels in Stage 3 with its strong reasoning and planning for long-text comprehension and comprehensive file configuration, its tendency to hallucinate or generate inaccuracies became a hurdle during development. These hallucinations led to problems such as misidentifying dimensional errors and inserting unwanted markdown formatting into corrected files, issues that extensive prompt engineering alone could not resolve.

To address these challenges, ChatCFD adopted a strategic hybrid method. In the case file correction module, DeepSeek-V3 now manages the majority of error corrections, which has markedly increased the success rate of these corrections. DeepSeek-R1 retains responsibility for resolving file-missing errors, as this task requires a holistic

analysis of all configuration files for consistency—a strength of DeepSeek-R1’s content processing. A similar division applies to error type identification: DeepSeek-V3 handles pattern-based errors like dimension and file-missing issues, while DeepSeek-R1 tackles complex errors, such as repetitive and common problems, which necessitate broader content analysis.

For DeepSeek-V3, the thought prompting by Wu et al. [35] in 2024 is used to equip DeepSeek-V3 with some thinking abilities. An auxiliary function then helps to extract the final answer from DeepSeek-V3’s response. The thought prompting text instructs the model to respond comprehensively and in detail, and to first write down its thought process after the phrase "Here is my thought process:" before providing its actual response after "Here is my response:". An example of thought prompting is given in Appendix C.

Furthermore, ChatCFD maintains a log of all Question-Answer (QA) histories with the LLMs for each CFD case. These QA logs are valuable for analyzing the LLM’s behavior as it configures CFD cases within the OpenFOAM framework.

The experimental validation detailed in Section 3 was conducted on the VolcEngine platform [31] from March 1 to March 12, 2025. The pricing structure for the models on this platform, used for evaluating token usage and cost, is as follows: for DeepSeek-R1, the cost is \$0.00055 (0.004 RMB) per 1,000 input tokens and \$0.0022 (0.016 RMB) per 1,000 output tokens; for DeepSeek-V3, the cost is \$0.00021 (0.0015 RMB) per 1,000 input tokens and \$0.00082 (0.006 RMB) per 1,000 output tokens. All token usage and cost calculations mentioned in Section 3 are based on this pricing structure from the VolcEngine platform.

3 Results and discussion

The performance of ChatCFD was assessed through validation experiments on basic CFD examples and two complex cases, using published literature as prompts. ChatCFD achieved error-free configurations in 30-40% of cases and operational success in 60-80%, marking a significant advance in automated CFD setup. The system demonstrated robust handling of complex configurations, particularly those with diverse turbulence models, highlighting its adaptability to varied physical scenarios. Analysis revealed two key performance factors: the extent of physical coupling in the flow and the availability of comprehensive knowledge about relevant physical models. These findings elucidate the capabilities and limitations of AI-driven CFD automation, contributing to the advancement of automated CFD workflows.

3.1 CFD cases for Experiments

We selected two representative test cases for simulation: an incompressible flow and a compressible flow case (illustrated in Figure 3). These cases were chosen based on the comprehensive documentation available in their source articles, which provided detailed specifications of the solver configurations, turbulence models, and mesh characteristics essential for accurate CFD reproduction. For the incompressible flow case, we utilized the work of Sun et al.[29], who conducted simulations of a NACA0012 airfoil at 10° angle of attack employing simpleFoam solver with the SpalartAllmaras turbulence model. For the compressible flow case, we referenced Yu et al.[36], who performed simulations of a nozzle with pressure ratio 3. The rhoCentralFoam and SpalartAllmaras model are used in the Nozzle case.

Given the documented challenges in modifying OpenFOAM turbulence models using LLM, as reported by Pandey et al.[25], we extended our investigation to include additional experiments with the NACA0012 case implementing various turbulence models. Table 1 presents a comprehensive overview of all case configurations and experimental iterations conducted in this study. High-quality computational meshes for these experiments were generated using commercial software. The experimental design featured a structured testing protocol: Cases 1 and 5 were subjected to an extensive model ablation analysis, with 10 iterations performed for each of the five system configurations. In contrast, Cases 2 through 4 were evaluated using only the complete system configuration, also with 10 iterations each. This systematic methodology yielded a total of 130 ChatCFD experimental runs, forming a robust dataset for subsequent analysis.

3.2 Model Ablation Analysis

To systematically evaluate the contributions of different components and strategies, ablation experiments were performed using five distinct system configurations. These configurations vary in terms of comprehensive paper interpretation detailed in Stage 2 (Initiating Case Files), the sophistication of error handling logic, and the utilization of retrieval modules (ReferenceRetriever and ContextRetriever) in Stage 3 (Correcting Case Files):

- **Configuration A (Baseline System):** Utilizes a simplified parameter extraction process instead of the three-step process in Stage 2. In Stage 3, error correction is limited to a basic “general error” pathway, with both ReferenceRetriever (tutorial-based retrieval) and ContextRetriever (current case retrieval) modules deactivated.

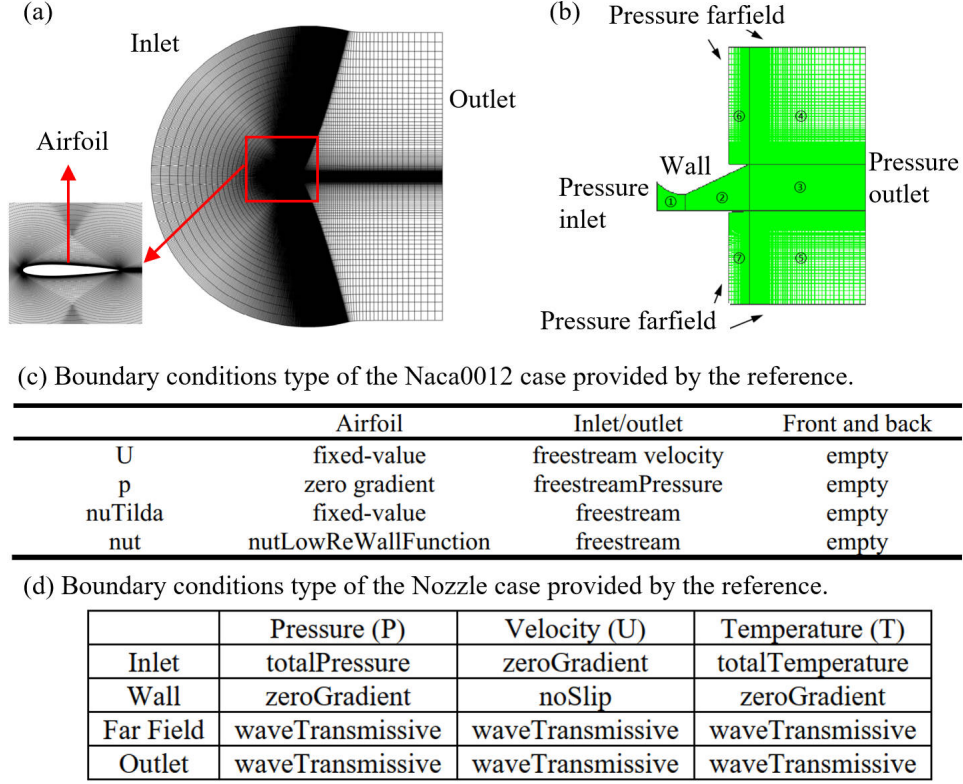


Figure 3: Demonstration of the two tested CFD cases, including grids of (a) the Naca0012 case [29] and (b) the Nozzle case [36], and boundary types of (c) the Naca0012 case and (d) the Nozzle case.

Table 1: Summary of Test Cases for ChatCFD Validation

Case ID	Case Mesh	Physical Models	Experimental Design
Case 1	NACA0012	simpleFoam with SpalartAllmaras	10 runs \times 5 system configurations
Case 2	NACA0012	simpleFoam with kOmegaSST	10 runs \times the complete system configuration
Case 3	NACA0012	simpleFoam with kEpsilon	10 runs \times the complete system configuration
Case 4	NACA0012	simpleFoam with RNGkEpsilon	10 runs \times the complete system configuration
Case 5	Nozzle	rhoCentralFoam with hePsiThermo and SpalartAllmaras	10 runs \times 5 system configurations

- **Configuration B (ReferenceRetriever with Basic Error Handling):** Maintains the simplified parameter extraction (Stage 2) and basic 'general error' handling (Stage 3) of Configuration A, but activates the ReferenceRetriever module to inform corrections with tutorial case data.
- **Configuration C (Multi-Category Errors, ReferenceRetriever, Simplified Extraction):** Employs the simplified parameter extraction in Stage 2. However, Stage 3 incorporates the full multi-category error correction logic (addressing dimensional, missing file, repetitive, and general errors) and activates the ReferenceRetriever module. The ContextRetriever module remains deactivated.

- **Configuration D (Multi-Category Errors, ReferenceRetriever & ContextRetriever, Simplified Extraction):** Also uses the simplified parameter extraction in Stage 2. Stage 3 employs the full multi-category error correction logic, supported by both ReferenceRetriever and ContextRetriever modules.
- **Configuration E (Complete System):** Represents the most comprehensive setup. It features comprehensive paper interpretation in Stage 2. In Stage 3, it utilizes the full multi-category error correction logic, augmented by both ReferenceRetriever and ContextRetriever modules.

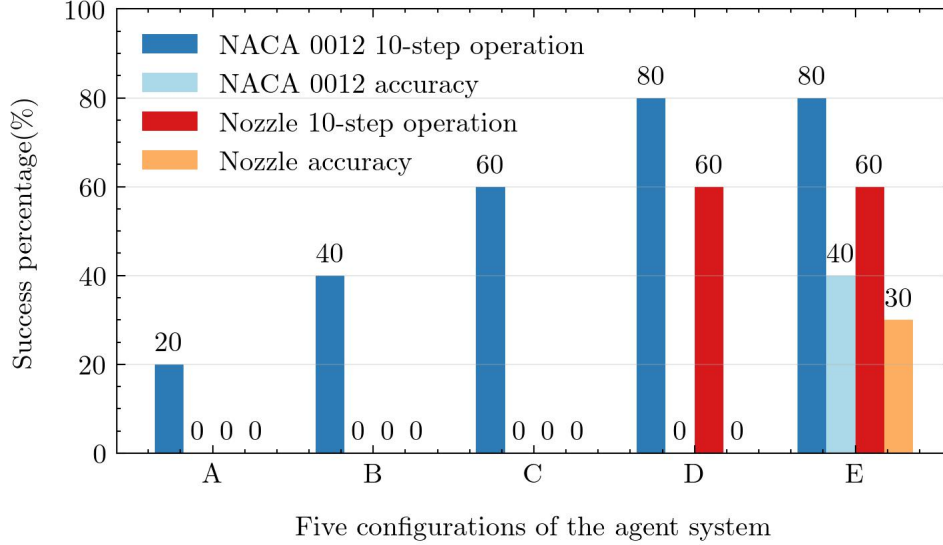


Figure 4: Success rates of ChatCFD in reproducing NACA0012 Case 1 and Nozzle Case 5 across five distinct Configurations A to E. The horizontal axis delineates these configurations, while the vertical axis quantifies the success rates. A 10-step operation indicates the CFD case successfully advanced 10 time steps or executed 10 iteration steps. Accuracy denotes precise case configuration in accordance with the source article’s specifications.

Figure 4 illustrates the performance of ChatCFD across the five distinct system Configurations A through E for two benchmark test cases: NACA0012 Case 1 and Nozzle Case 5. Two primary metrics were employed for evaluation: the *10-step operational success rate*, signifying the capability to complete ten simulation steps (time steps for transient cases or iterations for steady-state cases) without critical errors, and the *accurate configuration success rate*, indicating that the CFD case was set up in exact accordance with the specifications detailed in the source research article. The 10-step criterion was adopted to enable rapid assessment of operational stability for the system’s reflection mechanism, as target simulation durations are often unspecified in the literature. It was observed that configurations meeting this 10-step milestone were generally free of major operational faults, though minor discrepancies in boundary conditions parameters from the article’s description could still occur. For cases achieving accurate configuration, the simulation results demonstrated good agreement with published data, as detailed in Appendix D.

For the NACA0012 Case 1, the data in Figure 4 show a clear progression in the 10-step operational success rate with increasing system sophistication. The baseline Configuration A achieved a 20% success rate. This rate systematically improved to 40% for Configuration B, 60% for Configuration C, and reached 80% for Configuration D, which benefited from enhanced retrieval capabilities. This trend highlights the positive impact of incrementally integrating retrieval modules and OpenFOAM-specific knowledge. However, despite its high operational success, Configuration D failed to achieve any accurate configuration success, being unable to precisely replicate the case setup from the source article. This crucial gap was addressed by Configuration E, which incorporates comprehensive article interpretation and parameter extraction as part of its advanced Stage 2 processing. With Configuration E, the accurate configuration success rate for the NACA0012 case improved significantly to 40%, while maintaining the 80% operational success rate.

The comprehensive article interpretation module in Stage 2 is integral to achieving accurate CFD configurations, particularly for cases involving non-standard boundary conditions. For instance, the NACA0012 case, as depicted in Figure 3, employs several specialized OpenFOAM boundary conditions (freestream, freestreamVelocity, and freestreamPressure) that deviate from common practices. Analysis of the LLM’s internal reasoning processes indicated that, without robust article interpretation capabilities and strict adherence to documented specifications, the model tends

to default to more conventional boundary conditions. This can lead to erroneous configurations, such as using standard inlet-type conditions for inlet velocities and pressureOutlet-type conditions for outlet pressures, instead of the requisite specialized freestream conditions.

This tendency for conventional settings also extends to numerical parameters, including inlet velocity values. To mitigate these issues, the comprehensive article interpretation module was developed in Stage 2, incorporating a three-step process for analyzing articles. This process emphasizes the precise extraction of case specifications and ensures adherence to OpenFOAM’s inherent boundary condition types, as detailed in Section 2. The introduction of this module yielded substantial improvements: while the 80% success rate for the 10-step operational benchmark was maintained, the system’s capability to accurately replicate documented case configurations increased dramatically from 0% to 40%. This significant enhancement underscores the efficacy of the refined interpretation strategy in correctly identifying and implementing specialized case requirements.

In the Nozzle Case 5, as depicted in Figure 4, the introduction of the ContextRetriever module led to a substantial improvement in the 10-step operational success rate. Configurations lacking ContextRetriever (i.e., up to Configuration C) exhibited a 0% success rate for this metric. The integration of ContextRetriever in Configuration D elevated this rate to 60%. This marked improvement is attributed to ContextRetriever’s enhanced capability to diagnose and address complex coupling-related errors (refer to Appendix B for examples), a notable limitation in earlier configurations. For instance, when encountering thermophysical parameter errors in OpenFOAM (such as those related to Ψ , the compressibility), previous configurations often misidentified the error source as the constant/thermodynamicProperties file. However, such errors frequently originate from inconsistencies in the equation of state specifications within boundary condition entries in field files (e.g., 0/p or 0/T). The ContextRetriever module overcomes this by performing a comprehensive analysis across all relevant case directories (0/, constant/, and system/), thereby enabling more accurate error localization and effective correction strategies.

The differential performance of the ContextRetriever module when applied to the NACA0012 Case 1 and the Nozzle Case 5 can be attributed to fundamental distinctions in their underlying flow physics. NACA0012 Case 1, an incompressible flow simulation employing the pisoFoam solver, exhibits a comparatively weak coupling between pressure and velocity fields. In contrast, Nozzle Case 5, a compressible flow scenario utilizing the rhoCentralFoam solver, is characterized by strong interdependencies among density, temperature, and pressure, governed by the equation of state. The advanced analytical capabilities of ContextRetriever, particularly in discerning inter-file dependencies and identifying errors related to coupled physics, proved notably more effective for the Nozzle case due to its inherent complexities. While still beneficial, the module’s impact was less pronounced for the NACA0012 case, which features a less coupled system. This observed variance underscores the proficiency of ContextRetriever in managing comprehensive physical information across a spectrum of problem complexities.

Advancing from Configuration D to E for the Nozzle Case 5 preserved the 60% 10-step operational success rate while notably enhancing the accurate configuration success rate from 0% to 30%. This pattern of improvement in configuration precision, achieved by incorporating comprehensive article interpretation in Stage 2, mirrors the observations from the NACA0012 case, indicating a consistent benefit of the complete system configuration across different flow regimes.

Figure 5 presents a detailed analysis of the NACA0012 Case 1 performance across the five distinct Configurations (A through E), based on averaged results from 10-step operational success runs. This analysis yields several key insights into the system’s operational efficiency and cost-effectiveness.

The evolution of reflection iterations, illustrated in Figure 5(a), demonstrates an encouraging improvement pattern. As retrieve modules were integrated from configuration A to C, we observed a substantial decrease in required reflection iterations, followed by stabilization. This observation aligns with MetaOpenFOAM’s findings [6] regarding RAG positive impact on LLM response quality and CFD agent performance. The subsequent stability in reflection counts from configurations C to E suggests that additional RAG implementations, while beneficial for other aspects, had minimal impact on ChatCFD’s reflection behavior. This plateau is reasonable given that ContextRetriever and comprehensive paper interpretation modules were primarily designed to enhance performance on physical-coupled cases and setup accuracy respectively, rather than affecting reflection behaviors for weak coupling cases.

An analysis of token consumption and associated costs, depicted in Figure 5(b), reveals a pattern of improving resource utilization efficiency. Transitioning from Configuration A to D, while the token consumption of the DeepSeek-R1 model remained relatively stable, the DeepSeek-V3 model’s consumption decreased markedly. This reduction contributed to lower per-case operational costs (decreasing from \$0.078 to \$0.071). This cost improvement, concurrent with a significant increase in operational success rates from 20% to 80%, underscores the enhanced overall effectiveness of the ChatCFD system.

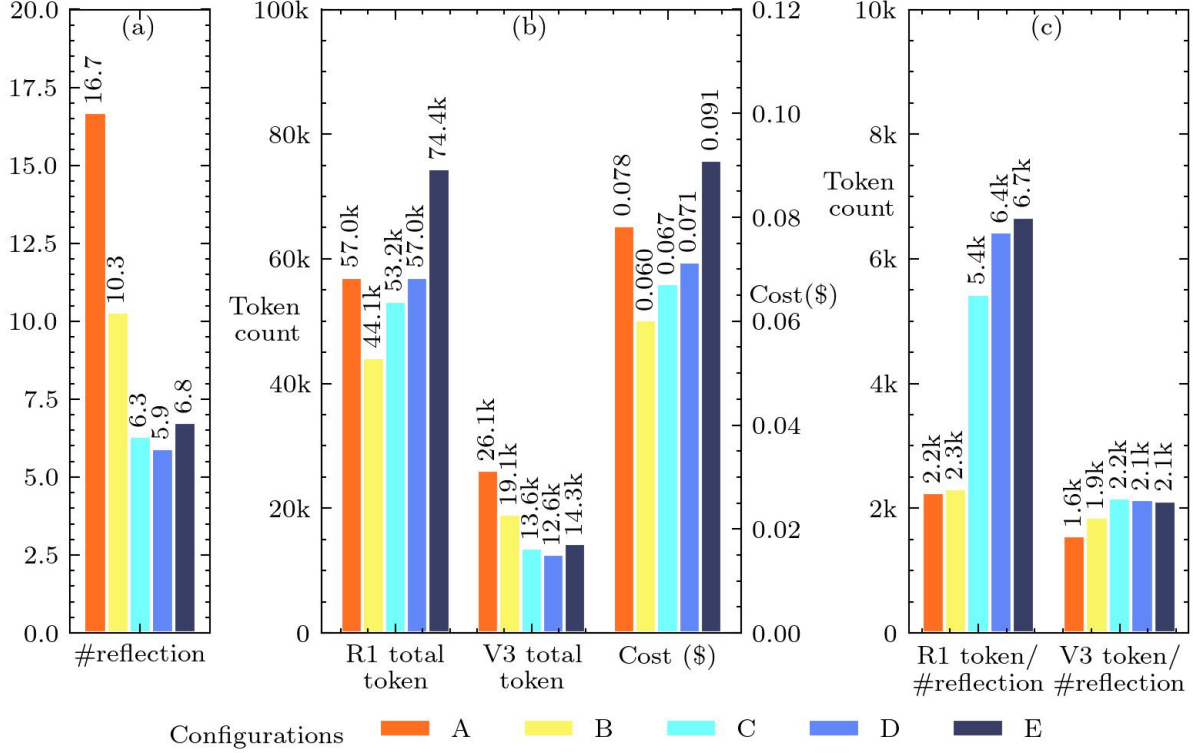


Figure 5: Results for NACA0012 Case 1 using Configurations A to E, showing averages of 10-step operational success runs. Metrics shown include: number of reflection iterations (#reflection), total token consumption for DeepSeek-R1 and DeepSeek-V3 models (R1/V3 total token), execution cost (Cost \$), and average token consumption per reflection round for both models (R1/V3 token/#reflection)

The transition from Configuration D to E resulted in a notable enhancement of system accuracy, as illustrated in Figure 4. This advancement was primarily achieved by improving the paper interpretation module’s efficacy in extracting CFD case setups during Stage 2 and by ensuring greater consistency of these setups throughout the file correction processes in Stage 3. Although this upgrade led to increased DeepSeek-R1 token consumption and a corresponding 30% rise in operational cost (from \$0.071 to \$0.091), the substantial improvement in accurate case configuration—from 0% to 40%—justifies this investment.

Figure 5(c) illustrates the token consumption patterns per reflection iteration for both DeepSeek-R1 and DeepSeek-V3 models across the different Configurations. From Configuration A to E, the DeepSeek-R1’s consumption increases to more than two times, where the increasing consumption are mostly due to the integration of the `ContextRetriever` module in Configuration C. The DeepSeek-V3’s consumption initially rose due to expanded error handling capabilities and reference case integration through `ReferenceRetriever`. The subsequent stabilization of DeepSeek-V3 token usage from Configuration C to E reflects the maturation of the reflection module’s design, achieving optimal operational efficiency without necessitating additional DeepSeek-V3 module invocations.

Figure 6 presents a comparative performance analysis for the Nozzle Case 5, specifically contrasting Configurations D and E, based on simulations that successfully completed ten steps. Configurations A through C were omitted from this comparison due to their inability to consistently reach this ten-step benchmark. The key differentiator between Configurations D and E is the integration of the comprehensive paper interpretation module’s enhanced article interpretation capabilities in Configuration E. Notwithstanding this enhancement, Figure 6(a) indicates that the number of reflection iterations remained largely comparable between these two configurations, with only marginal reductions observed for Configuration E.

The deployment of comprehensive paper interpretation module resulted in increased token utilization, as depicted in Figure 6(b). Configuration E demonstrated higher token consumption by the DeepSeek-R1 model, whereas the DeepSeek-V3 model’s token usage remained stable across both Configurations D and E. In terms of operational

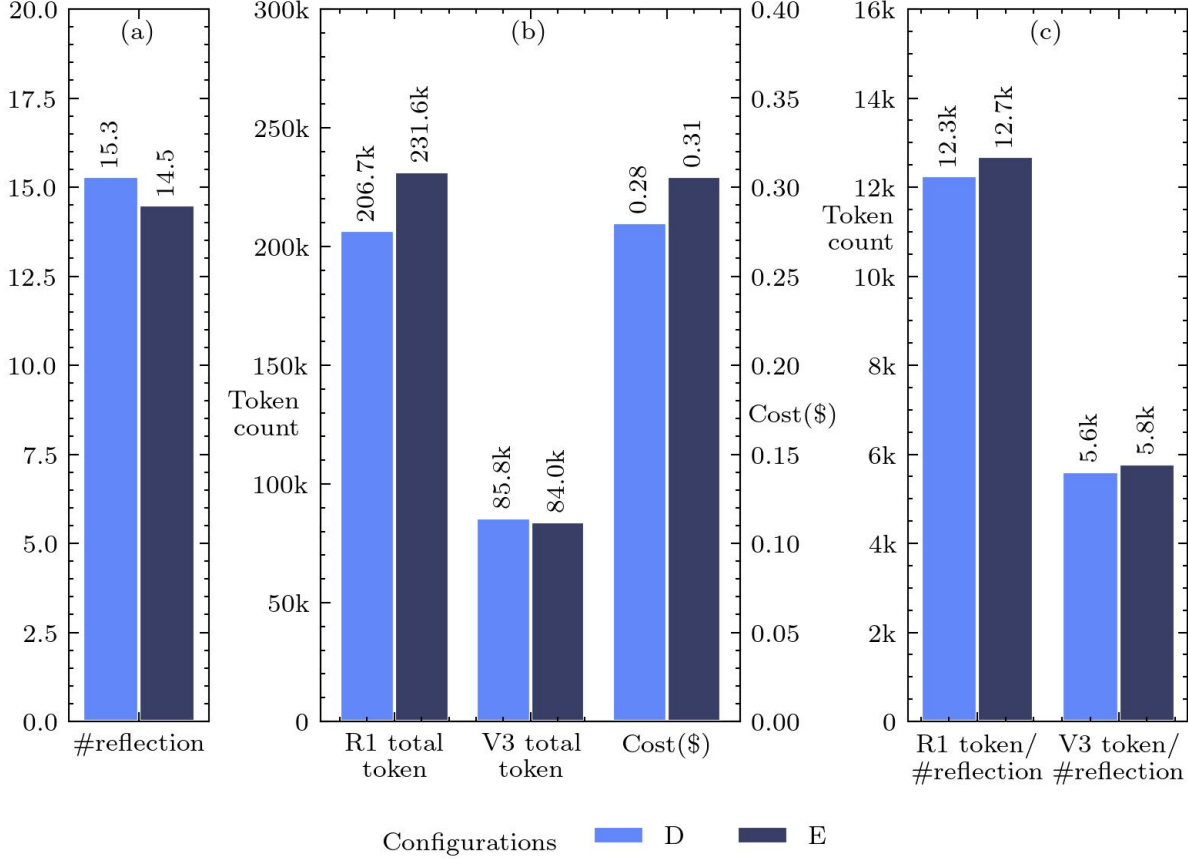


Figure 6: Results for Nozzle Case 5 using Configurations D and E, showing averages of 10-step operational success runs. Metrics shown include: number of reflection iterations (#reflection), total token consumption for DeepSeek-R1 and DeepSeek-V3 models (R1/V3 total token), execution cost (Cost \$), and average token consumption per reflection round for both models (R1/V3 token/#reflection)

cost, the average per-case expenditure saw a modest increase from \$0.28 to \$0.31, an approximate 10% increment. Nevertheless, this additional investment yielded significant improvements in performance, particularly in case setup accuracy, which, as shown in Figure 4, rose substantially from 0% to 30%.

Further examination, illustrated in Figure 6(c), reveals that the average token consumption per reflection iteration for both the DeepSeek-R1 and DeepSeek-V3 models was comparable across Configurations D and E. This consistency underscores the efficacy of the system’s architectural design, indicating that the comprehensive paper interpretation module detailed interpretation component operates as a distinct layer that augments overall system performance without adversely affecting the fundamental reflection mechanisms.

3.3 Performance degradation in configuring physical-coupled CFD cases

The model ablation analysis in Section 3.2 highlights significant performance variations among configurations A through E when applied to two distinct test cases: the incompressible NACA0012 Case 1 and the compressible Nozzle Case 5. These discrepancies are attributed to fundamental differences in their underlying flow physics, with subsequent discussion detailing the influence of physical coupling—a key characteristic of compressible flow prominent in the Nozzle case—on ChatCFD’s performance.

The Nozzle case utilizes the `rhoCentralFoam` solver, which inherently manages strong interdependencies between pressure, temperature, and density through its thermophysical models. Its compressible flow solution also dictates supersonic or subsonic conditions based on local velocity and sound speed, which are coupled with thermodynamic properties (e.g., pressure, temperature). In contrast, the NACA0012 case employs the `simpleFoam` solver, featuring minimal such coupling. As shown in Table 2, these differing physical complexities translate to substantially different

Table 2: Statistical averages of accurate configured cases for Naca0012 Case 1 and Nozzle Case 5.

Metrics	Naca0012, Case 1	Nozzle, Case 5
Physical models	Flow type: Incompressible Solver: simpleFoam Turbulence: SpalartAllmaras	Flow type: Compressible Solver: rhoCentralFoam Turbulence: SpalartAllmaras Thermo model: hePsiThermo
Number of configuration files	9	12
Average tokens for all configuration files per case	1,792	2,647
Configuration files	0/p 0/U 0/nut 0/nuTilda constant/transportProperties constant/turbulenceProperties system/controlDict system/fvSchemes system/fvSolution	0/p 0/U 0/nut 0/nuTilda 0/T 0/alphat constant/transportProperties constant/turbulenceProperties constant/thermodynamicProperties system/controlDict system/fvSchemes system/fvSolution
DeepSeek-R1 call count	19.1	48.3
DeepSeek-V3 call count	17.4	35.2

configuration requirements. The Nozzle case demands more configuration files with greater token content and three additional thermophysical-related files (0/T, 0/alphat, constant/thermodynamicProperties). Furthermore, achieving a precise configuration for this compressible flow scenario necessitates over twice the DeepSeek-R1 and DeepSeek-V3 model calls compared to the incompressible NACA0012 case.

Section 3.2 results demonstrate that the strong physical coupling in the Nozzle case correlates with diminished success rates. Figure 4 illustrates this, showing that the highly coupled Nozzle case consistently achieves lower 10-step success and precise configuration rates across ten experimental runs. This performance degradation is attributed to two primary factors: the increased complexity of managing a larger number of files with more extensive content, and the stringent requirement for maintaining consistency across interconnected thermophysical models and related parameters (e.g., in files such as 0/p, 0/T, and constant/thermodynamicProperties).

The greater physical complexity of the Nozzle case translates directly to substantially higher LLM consumptions than NACA0012 Case 1 (Figure 7). Specifically, the Nozzle simulation requires over double the reflection iterations for convergence, consumes approximately triple the total DeepSeek-R1 tokens, and uses six times the DeepSeek-V3 tokens. These escalated resource needs lead to the Nozzle case incurring roughly triple the operational costs. Such pronounced differences in resource utilization directly quantify the greater computational burden imposed by the strong physical coupling in compressible flow simulations relative to their incompressible counterparts.

Notably, the DeepSeek-V3 token consumption for the Nozzle case increased by a factor of approximately six, substantially exceeding the DeepSeek-R1 token increase of approximately threefold. Analysis of case execution QA histories reveals this disparity stems from a higher incidence of dimensional inconsistencies and persistent errors during Nozzle case configuration, which in turn necessitated more frequent invocations of the DeepSeek-V3 model. Figure 7(c) corroborates this, showing that the per-reflection DeepSeek-V3 token multiplier for the Nozzle case (about 2.7x) is obviously larger than its DeepSeek-R1 multiplier (about 2x) compared to the NACA0012 case.

The analysis of dimensional errors reveals a notably higher frequency in compressible flow scenarios, such as the Nozzle case, attributable to two fundamental factors. First, compressible flow physics imposes inherently more stringent

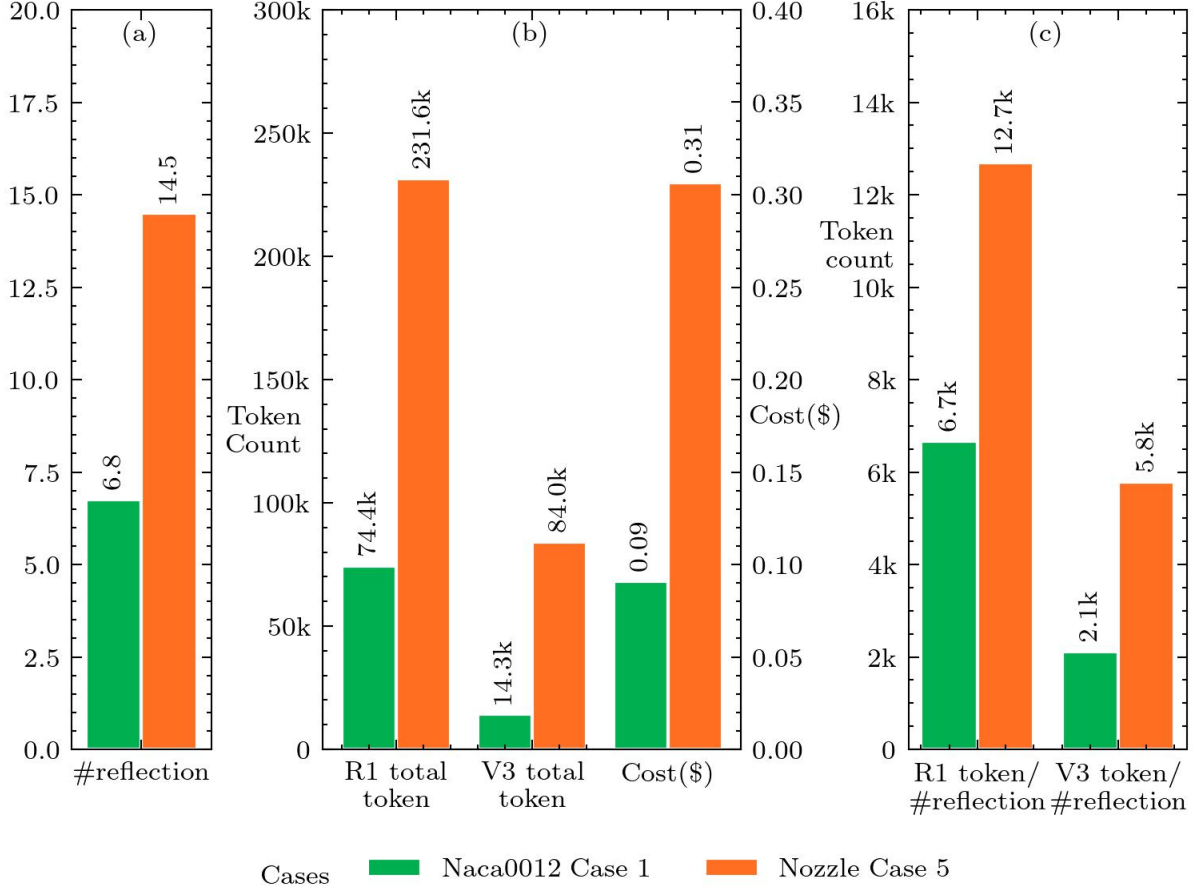


Figure 7: ChatCFD’s average performance per execution when accurately configuring NACA0012 Case 1 and Nozzle Case 5. Metrics shown include: number of reflection iterations (#reflection), total token consumption for DeepSeek-R1 and DeepSeek-V3 models (R1/V3 total token), execution cost (Cost \$), and average token consumption per reflection round for both models (R1/V3 token/#reflection).

requirements for achieving consistent setups; this involves not only the dimensional consistency and intricate coupling of primary fields like pressure, density, and velocity, but critically, their coherent integration with a thermodynamic model (such as an equation of state). This model, which interrelates these variables, often via temperature and specific energy, demands precise dimensional and physical alignment across all governing equations and material property definitions, a level of rigor that significantly elevates the complexity compared to typical incompressible simulations. Second, and significantly, the predominant focus on incompressible flow applications in typical CFD scenarios appears to have created an implicit bias in LLM training data. This bias manifests as a tendency for the LLM to default to incompressible flow configurations, even when handling compressible cases. A pertinent example of how this bias can degrade compressible flow configurations is the differing treatment of pressure dimensions: in OpenFOAM, incompressible flows often implement kinematic pressure p_k , which is dynamic pressure over density and has dimensions of L^2T^{-2} whereas compressible flows use absolute dynamic (thermodynamic) pressure (p) with dimensions $ML^{-1}T^{-2}$. An LLM incorrectly applying the incompressible pressure dimension convention to a compressible case due to this training bias would introduce a fundamental dimensional error. Consequently, when LLMs encounter compressible flow scenarios, these embedded assumptions can lead to dimensional errors, exemplified by the pressure dimension mismatch, that require additional correction cycles to resolve.

3.4 Effects of turbulence models on ChatCFD’s performance

Figure 8 presents a detailed performance analysis of ChatCFD across four distinct turbulence models—Spalart-Allmaras (SA), kEpsilon, kOmegaSST, and RNGkEpsilon—applied to the NACA0012 benchmark (Cases 1 to 4). The evaluation focuses on simulations that achieved accurate configuration in accordance with published literature specifications,

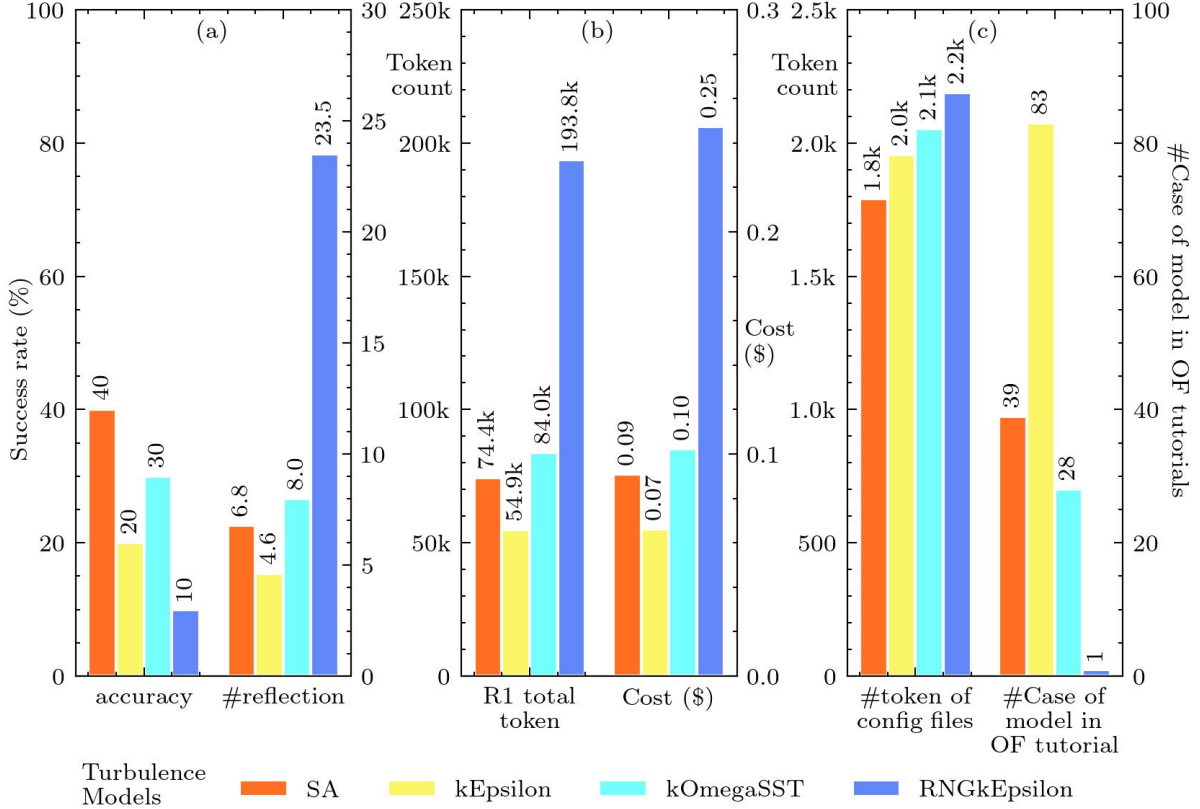


Figure 8: ChatCFD’s performance when applying four turbulence models to the NACA0012 Cases 1 to 4, where the results represent the average outcomes of cases precisely configured according to the paper specifications. The turbulence models include SpalartAllmaras, kEpsilon, kOmegaSST, and RNGkEpsilon. Metrics shown include: accuracy (success rate of precise configuration according to literature), number of reflection iterations (#reflection), total token consumption of the DeepSeek-R1 model (R1 total token), execution cost (Cost \$), token count of configuration files (#token of config files), and the number of cases incorporating each turbulence model in OpenFOAM tutorials (#Case of model in OF tutorial).

thereby excluding instances that only demonstrated rudimentary operational functionality (i.e., 10-step operational success). All experimental results reported herein were obtained using Configuration E, representing the complete agentic system.

As illustrated in Figure 8(a), the analysis reveals distinct success rates for accurate case configuration across the four turbulence models. The SA model achieved the highest success rate at 40%, followed by the kOmegaSST model (30%) and the kEpsilon model (20%). The RNGkEpsilon model exhibited markedly lower performance, with a success rate of 10%. Notably, while OpenFOAMGPT [25] has underscored the difficulties LLMs encounter when modifying turbulence models during case configuration, ChatCFD’s capability to successfully implement all four models attests to its efficacy in addressing these challenges, thereby validating the proposed architectural design and implementation methodology.

A detailed comparison of performance metrics, presented in Figure 8(a,b), delineates a clear behavioral divergence. The SA, kEpsilon, and kOmegaSST models displayed consistent performance profiles, characterized by an average reflection count of approximately 6, alongside comparable DeepSeek-R1 token utilization and associated computational expenditures. Conversely, the RNGkEpsilon model demanded substantially greater computational resources, evidenced by an average reflection count of 23.5—nearly fourfold higher than the other models—leading to correspondingly elevated token consumption and operational costs.

To elucidate the origins of these performance disparities, an analysis of underlying factors was conducted, with results presented in Figure 8(c). This investigation considered both the token counts of configuration files and the prevalence of each turbulence model within the OpenFOAM tutorial suite. Although configuration file sizes exhibited only modest

variations—the SA model requiring around 1,800 tokens compared to approximately 2,000 for the others—this minor difference is insufficient to account for the substantial performance gap. A more significant factor emerged from the distribution of tutorial cases: whereas the SA, kEpsilon, and kOmegaSST models were each featured in 28 or more tutorial examples, the RNGkEpsilon model was represented in merely one instance.

The pronounced performance deficit observed for the RNGkEpsilon model is attributable to two principal factors. Firstly, its relative infrequency in practical engineering applications translates to a scarcity of representative examples in the LLM’s training dataset. This limitation impairs the LLM’s proficiency in configuring RNGkEpsilon cases effectively in a zero-shot manner (i.e., without RAG). Secondly, the model’s minimal presence within the OpenFOAM tutorials severely curtails the efficacy of the ReferenceRetriever module in sourcing appropriate reference configurations from this dataset. This is particularly detrimental for RNGkEpsilon-specific parameters, such as those found in the `constant/turbulenceProperties` file and associated numerical schemes within `system/fvSchemes` and `system/fvOptions`. This dearth of tutorial-based guidance necessitates a greater dependence on the LLM’s intrinsic, yet less developed, understanding of the RNGkEpsilon model, culminating in diminished performance relative to more ubiquitously employed turbulence models.

4 Conclusion

This paper introduced ChatCFD, an innovative LLM-based CFD agent system designed to automate CFD simulations within the OpenFOAM framework. By integrating a multi-agent architecture, domain-specific knowledge bases, and advanced error correction mechanisms, ChatCFD successfully demonstrates the feasibility of end-to-end automation for both incompressible (NACA0012 airfoil) and compressible (supersonic nozzle) flow cases. Compared with antecedent CFD agent systems, such as MetaOpenFOAM [5] and OpenFOAMGPT [25], ChatCFD distinguishes itself through several key innovations:

Firstly, ChatCFD advances the application paradigm of LLM agents in engineering simulation through an interactive guidance mechanism that innovatively integrates multimodal inputs—PDF files, mesh files, and interactive dialogue—with underlying physical constraints. This mechanism, featuring a dedicated mesh input module and a reinforced context-memory dialogue system, offers a ChatGPT-like interface. This interface systematically guides users through essential stages, including literature analysis, case selection, the uploading of user-defined meshes, and the interactive specification of CFD model parameters, thereby addressing the complexities inherent in practical CFD applications. Consequently, this approach substantially reduces operational hurdles compared to traditional command-line driven methodologies.

Secondly, the system employs a collaborative framework of specialized AI agents that leverage deep CFD domain expertise. This strategy involves: (a) a comprehensive article interpretation module, utilizing an advanced reasoning LLM (e.g., DeepSeek-R1), for extracting CFD case parameters (e.g., boundary names, types, values) from academic papers, augmented by extensive OpenFOAM-specific boundary condition information to mitigate model hallucination, which is vital for precise CFD case replication; (b) preprocessing data from OpenFOAM tutorial cases to construct comprehensive feature libraries, thereby enriching the system’s understanding through RAG; and (c) a "global planning-local optimization" hierarchical framework. This framework strategically synergizes the advanced reasoning and text interpretation capabilities of one LLM with the high-fidelity, low-hallucination file modification strengths of another. For instance, when correcting configuration errors, DeepSeek-R1 first analyzes error messages and relevant files to pinpoint the erroneous file and suggest corrections, which DeepSeek-V3 then implements, ensuring both accuracy and reliability.

Thirdly, ChatCFD features a powerful multi-category error correction mechanism with two specialized RAG modules: ReferenceRetriever (accessing tutorial templates) and ContextRetriever (collecting current case configurations). This feature actively monitors simulation outputs in real-time, dynamically selecting appropriate and effective treatments by classifying typical case configuration problems. These include, but are not limited to, dimensional inconsistencies, missing file errors, and recurring errors indicative of deeper setup issues, thereby systematically addressing critical logical consistency challenges frequently encountered by LLMs in complex CFD computations.

Systematic ablation studies and case validations underscored the critical contributions of ChatCFD’s components. Comprehensive paper interpretation proved paramount for achieving high configurational accuracy, particularly for cases with rare or non-standard boundary conditions (e.g., “freestream” for NACA0012), improving accurate configuration success from 0% to 40% for the NACA0012 case and from 0% to 30% for the Nozzle case. The ContextRetriever module, which provides contextual awareness of current case files, was especially vital for diagnosing and rectifying complex, physically-coupled errors in compressible flow simulations; this boosted the Nozzle case’s 10-step operational success rate from 0% to 60%. Overall, the system achieved accurate configuration for approximately 30-40% of tested scenarios directly from literature, with higher operational success rates (e.g., 80% for NACA0012 with full system

capabilities), establishing a valuable performance benchmark. Furthermore, the study quantified the cost-effectiveness of different system configurations. For instance, a 30% cost increase yielded a 40% improvement in accurate configuration for the NACA0012 case, justifying the investment for enhanced precision. These results highlight that while LLMs can automate aspects of CFD, their efficacy is significantly amplified when augmented with structured domain knowledge and robust error-handling mechanisms.

Key findings indicate that ChatCFD’s performance is significantly impacted by the complexity and representation of CFD cases in its knowledge base. Configuring physically-coupled compressible flow scenarios, like the Nozzle case, drastically degrades performance compared to incompressible ones due to more numerous and intricate configuration files and the critical need for consistency across interdependent thermophysical parameters. This results in lower success rates for accurate configurations, substantially increased LLM calls, higher token consumption (especially for error correction by DeepSeek-V3), more reflection iterations, and tripled operational costs, with dimensional errors exacerbated by the inherent rigor of compressible physics and an LLM training bias towards incompressible flow conventions. Similarly, performance varies markedly with the chosen turbulence model; those well-represented in OpenFOAM tutorials (e.g., Spalart-Allmaras with 40% success) yield better results and lower resource use. In contrast, models like RNGkEpsilon, scarce in both general LLM training data and specific tutorial datasets (only one example), exhibit poor success (10%) and demand significantly more computational resources, underscoring how limited data representation hampers ChatCFD’s configuration proficiency and RAG effectiveness.

ChatCFD pioneers computational automation, extending LLM applications to engineering challenges. By reducing expertise and software barriers, it democratizes access to advanced methodologies, fostering innovation. Its approaches—structured knowledge integration and context-aware RAG—offer insights for AI-driven engineering domains, such as simulations and optimizations. Future work includes expanding the knowledge base and developing standardized metrics to enhance automation, paving the way for AI-assisted scientific discovery.

ACKNOWLEDGEMENTS

This work is sponsored by the National Natural Science Foundation of China Grant No. 92470127, 92270203, the Open Project of the National Key Laboratory of Scramjet Technology No. WZC6142703202403, and the Overseas Postdoctoral Talents Program in Guangdong.

AUTHOR DECLARATIONS

Conflict of Interest

The authors declare no conflicts of interest.

Author Contributions

E Fan: Methodology, Software, Data curation, Formal analysis, Resources, Writing - original draft.

Weizong Wang: Resources, Funding acquisition.

Tianhan Zhang: Conceptualization, Methodology, Formal analysis, Resources, Writing - Review & Editing, Visualization, Supervision, Funding acquisition

Data Availability

The data that support the findings of this study are available from the corresponding author upon reasonable request.

References

- [1] Josh Achiam, Steven Adler, Sandhini Agarwal, Lama Ahmad, Ilge Akkaya, Florencia Leoni Aleman, Diogo Almeida, Janko Altenschmidt, Sam Altman, Shyamal Anadkat, et al. Gpt-4 technical report. *arXiv preprint arXiv:2303.08774*, 2023.
- [2] Joseph Amponsah, Emmanuel Adorkor, David Ohene Adjei Opoku, Anthony Ayine Apatika, and Vincent Nyanzu Kwofie. Computational modeling of hydrogen behavior and thermo-pressure dynamics for safety assessment in nuclear power plants. *Physics of Fluids*, 36(12), 2024.
- [3] John David Anderson and John Wendt. *Computational fluid dynamics*, volume 206. Springer, 1995.

- [4] Jiri Blazek. *Computational fluid dynamics: principles and applications*. Butterworth-Heinemann, 2015.
- [5] Yuxuan Chen, Xu Zhu, Hua Zhou, and Zhuyin Ren. Metaopenfoam: an llm-based multi-agent framework for cfd. *arXiv preprint arXiv:2407.21320*, 2024.
- [6] Yuxuan Chen, Xu Zhu, Hua Zhou, and Zhuyin Ren. Metaopenfoam 2.0: Large language model driven chain of thought for automating cfd simulation and post-processing. *arXiv preprint arXiv:2502.00498*, 2025.
- [7] Mohammad Ali Daeian, W Spencer Smith, and Zahra Keshavarz-Motamed. A multi-domain lattice boltzmann mesh refinement method for non-newtonian blood flow modeling. *Physics of Fluids*, 37(1), 2025.
- [8] Zhehao Dong, Zhen Lu, and Yue Yang. Fine-tuning a large language model for automating computational fluid dynamics simulations. *Theoretical and Applied Mechanics Letters*, page 100594, 2025.
- [9] Siamak N Doost, Dhanjoo Ghista, Boyang Su, Liang Zhong, and Yosry S Morsi. Heart blood flow simulation: a perspective review. *Biomedical engineering online*, 15:1–28, 2016.
- [10] E Fan, Jiaao Hao, Ben Guan, Chih-yung Wen, and Lisong Shi. Numerical investigation on reacting shock-bubble interaction at a low mach limit. *Combustion and Flame*, 241:112085, 2022.
- [11] E Fan, Weizong Wang, and Tianhan Zhang. Numerical investigation on flame dynamic and regime transitions during shock-cool flame interaction. *Combustion and Flame*, 273:113928, 2025.
- [12] Jianhui Fan, Jiaao Hao, and Chih-Yung Wen. Nonlinear interactions of global instabilities in hypersonic laminar flow over a double cone. *Physics of Fluids*, 34(12), 2022.
- [13] Daya Guo, Dejian Yang, Haowei Zhang, Junxiao Song, Ruoyu Zhang, Runxin Xu, Qihao Zhu, Shirong Ma, Peiyi Wang, Xiao Bi, et al. Deepseek-r1: Incentivizing reasoning capability in llms via reinforcement learning. *arXiv preprint arXiv:2501.12948*, 2025.
- [14] Jiaao Hao, Shibin Cao, Chih-Yung Wen, and Herbert Olivier. Occurrence of global instability in hypersonic compression corner flow. *Journal of Fluid Mechanics*, 919:A4, 2021.
- [15] Sirui Hong, Xiawu Zheng, Jonathan Chen, Yuheng Cheng, Jinlin Wang, Ceyao Zhang, Zili Wang, Steven Ka Shing Yau, Zijuan Lin, Liyang Zhou, et al. Metagpt: Meta programming for multi-agent collaborative framework. *arXiv preprint arXiv:2308.00352*, 3(4):6, 2023.
- [16] Edward J Hu, Yelong Shen, Phillip Wallis, Zeyuan Allen-Zhu, Yuanzhi Li, Shean Wang, Lu Wang, Weizhu Chen, et al. Lora: Low-rank adaptation of large language models. *ICLR*, 1(2):3, 2022.
- [17] Alfredo Iranzo. Cfd applications in energy engineering research and simulation: an introduction to published reviews. *Processes*, 7(12):883, 2019.
- [18] Hrvoje Jasak, Aleksandar Jemcov, Zeljko Tukovic, et al. Openfoam: A c++ library for complex physics simulations. In *International workshop on coupled methods in numerical dynamics*, volume 1000, pages 1–20. Dubrovnik, Croatia), 2007.
- [19] Yu-Hsuan Juan, Vita Ayu Aspriyanti, and Wan-Yi Chen. Wind flow characteristics in high-rise urban street canyons with skywalks. *Physics of Fluids*, 37(3), 2025.
- [20] Jyotsna Balakrishna Kodman, Balbir Singh, and Manikandan Murugaiah. A comprehensive survey of open-source tools for computational fluid dynamics analyses. *J. Adv. Res. Fluid Mech. Therm. Sci*, 119:123–148, 2024.
- [21] Patrick Lewis, Ethan Perez, Aleksandra Piktus, Fabio Petroni, Vladimir Karpukhin, Naman Goyal, Heinrich Küttler, Mike Lewis, Wen-tau Yih, Tim Rocktäschel, et al. Retrieval-augmented generation for knowledge-intensive nlp tasks. *Advances in neural information processing systems*, 33:9459–9474, 2020.
- [22] Zhengtong Li, Tingzhen Ming, Shurong Liu, Chong Peng, Renaud de Richter, Wei Li, Hao Zhang, and Chih-Yung Wen. Review on pollutant dispersion in urban areas-part a: Effects of mechanical factors and urban morphology. *Building and Environment*, 190:107534, 2021.
- [23] Yue Ling, Somasekharan Nithin, Cao Yadi, and Pan Shaowu. Foam-agent: Towards automated intelligent cfd workflows. *arXiv preprint arXiv:2505.04997*, 2025.
- [24] Paul D Morris, Andrew Narracott, Hendrik von Tengg-Kobligk, Daniel Alejandro Silva Soto, Sarah Hsiao, Angela Lungu, Paul Evans, Neil W Bressloff, Patricia V Lawford, D Rodney Hose, et al. Computational fluid dynamics modelling in cardiovascular medicine. *Heart*, 102(1):18–28, 2016.
- [25] Sandeep Pandey, Ran Xu, Wenkang Wang, and Xu Chu. Openfoamgpt: A retrieval-augmented large language model (llm) agent for openfoam-based computational fluid dynamics. *Physics of Fluids*, 37(3), 2025.
- [26] Stefan Posch, Clemens Gößnitzer, Michael Lang, Ricardo Novella, Helfried Steiner, and Andreas Wimmer. Turbulent combustion modeling for internal combustion engine cfd: A review. *Progress in Energy and Combustion Science*, 106:101200, 2025.

- [27] Lian Shen, Yan Han, CS Cai, Peng Hu, Xu Lei, Pinhan Zhou, and Shuwen Deng. Equilibrium atmospheric boundary layer model for numerical simulation of urban wind environment. *Physics of Fluids*, 36(8), 2024.
- [28] Jeffrey P Slotnick, Abdollah Khodadoust, Juan Alonso, David Darmofal, William Gropp, Elizabeth Lurie, and Dimitri J Mavriplis. Cfd vision 2030 study: a path to revolutionary computational aerosciences. Technical report, NASA, 2014.
- [29] Zhaozheng Sun and Wenhui Yan. Comparison of different turbulence models in numerical calculation of low-speed flow around naca0012 airfoil. In *Journal of Physics: Conference Series*, page 012075. IOP Publishing, 2023.
- [30] Gemini Team, Rohan Anil, Sebastian Borgeaud, Jean-Baptiste Alayrac, Jiahui Yu, Radu Soricut, Johan Schalkwyk, Andrew M Dai, Anja Hauth, Katie Millican, et al. Gemini: a family of highly capable multimodal models. *arXiv preprint arXiv:2312.11805*, 2023.
- [31] VolcEngine. VolcEngine - A Cloud Service Platform by ByteDance. <https://www.volcengine.com/>, 2025. Accessed: May 8, 2025.
- [32] Haixin Wang, Yadi Cao, Zijie Huang, Yuxuan Liu, Peiyan Hu, Xiao Luo, Zezheng Song, Wanjia Zhao, Jilin Liu, Jinan Sun, et al. Recent advances on machine learning for computational fluid dynamics: A survey. *arXiv preprint arXiv:2408.12171*, 2024.
- [33] Jason Wei, Xuezhi Wang, Dale Schuurmans, Maarten Bosma, Fei Xia, Ed Chi, Quoc V Le, Denny Zhou, et al. Chain-of-thought prompting elicits reasoning in large language models. *Advances in neural information processing systems*, 35:24824–24837, 2022.
- [34] Qingyun Wu, Gagan Bansal, Jieyu Zhang, Yiran Wu, Beibin Li, Erkang Zhu, Li Jiang, Xiaoyun Zhang, Shaokun Zhang, Jiale Liu, et al. Autogen: Enabling next-gen llm applications via multi-agent conversation. *arXiv preprint arXiv:2308.08155*, 2023.
- [35] Tianhao Wu, Janice Lan, Weizhe Yuan, Jiantao Jiao, Jason Weston, and Sainbayar Sukhbaatar. Thinking llms: General instruction following with thought generation. *arXiv preprint arXiv:2410.10630*, 2024.
- [36] T Yu, Y Yu, YP Mao, YL Yang, and SL Xu. Comparative study of openfoam solvers on separation pattern and separation pattern transition in overexpanded single expansion ramp nozzle. *Journal of Applied Fluid Mechanics*, 16(11):2249–2262, 2023.